BERKELEY LAB

LAWRENCE BERKELEY NATIONAL LABORATORY

U.S. DEPARTMENT OF ENERGY

Experimental Measurement and Analysis of Insert Debonding in Carbon Fiber Structures for Particle Detectors

M. Janda[1], G. Vallone[2], E. Anderssen[2], D. Boettcher[2], T. Johnson[2], C. Bird[2], T. Claybaugh[2], M. McGee Toledo[2]

[1]CTU in Prague, Czech Republic

[2]Lawrence Berkeley National Laboratory, Berkeley, California

Forum on Tracker Detector Mechanics 2023

31 May 2023

Outline

- Introduction
- The ATLAS Inner Tracker Design
- Experimental Design Verification
- Debonding models
- Conclusion

Outline

- Introduction
- The ATLAS Inner Tracker Design
- Experimental Design Verification
- Debonding models
- Conclusion

Introduction

- **Composite structures** for tracker detectors target high stiffness to ensure precise positioning and good stability of the sensing elements

- Structural connections rely on glued and bolted connections
  - **Glued** connections can provide high stiffness and strength, but can limit the **flexibility** during assembly
  - **Bolted** connections provide high strength, but can allow relative motions between the connected components
  - Often, the stiffness and strength of critical connections is verified experimentally

- Predicting the **strength** of glued joints can be challenging:
  - Conservative estimates allow to dimension the structure
  - Advanced models required to predict the failure point with higher precision

- Here, we present numerical and analytical **models** of bonded inserts, comparing their results with the available **measurements**

Outline

- Introduction
- The ATLAS Inner Tracker Design
- Experimental Design Verification
- Debonding models
- Conclusion

ITk - Global Mechanics

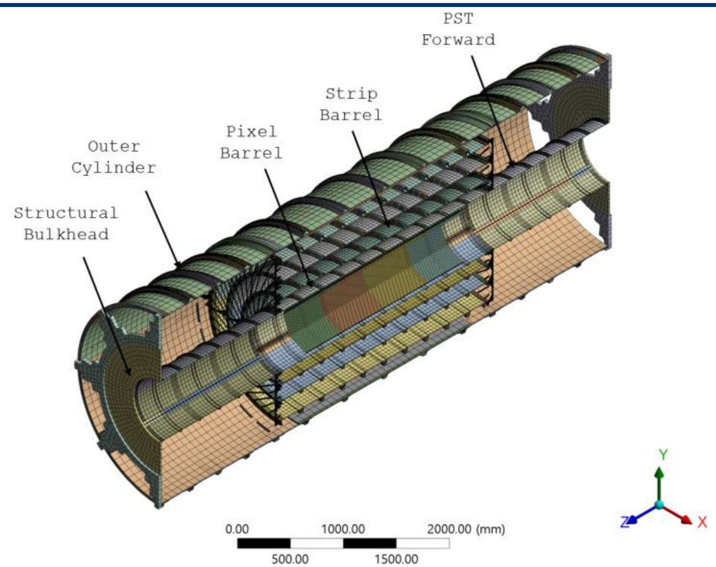

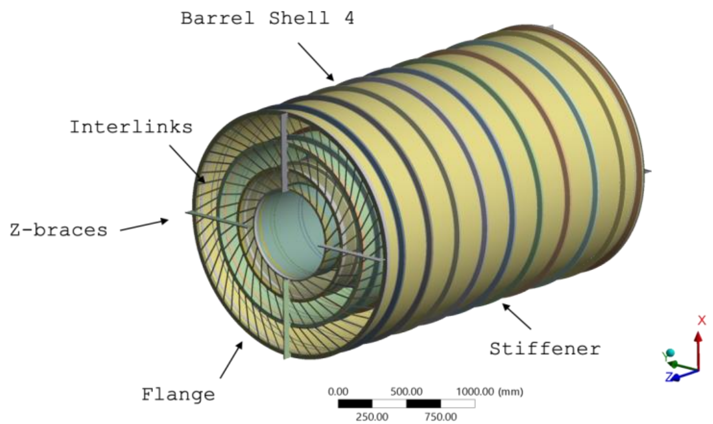

- **Global** ITk **structure** uses thin carbon fiber reinforced **laminates**, eccentrically **stiffened**
  - Design relies extensively on finite element modeling
  - **Stability** performance inversely proportional to the **gravity sag** of the system. Requirement: ~ < 2 mm
    - Total vertical sag: 850 μm under 3 tons

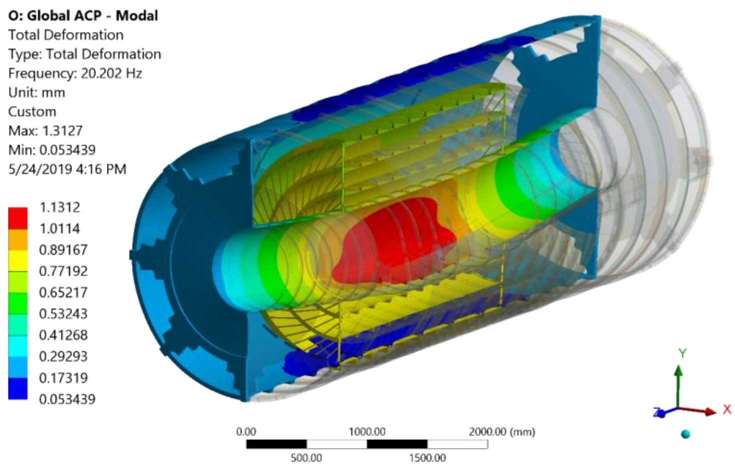

Experimental Tests - Stiffness

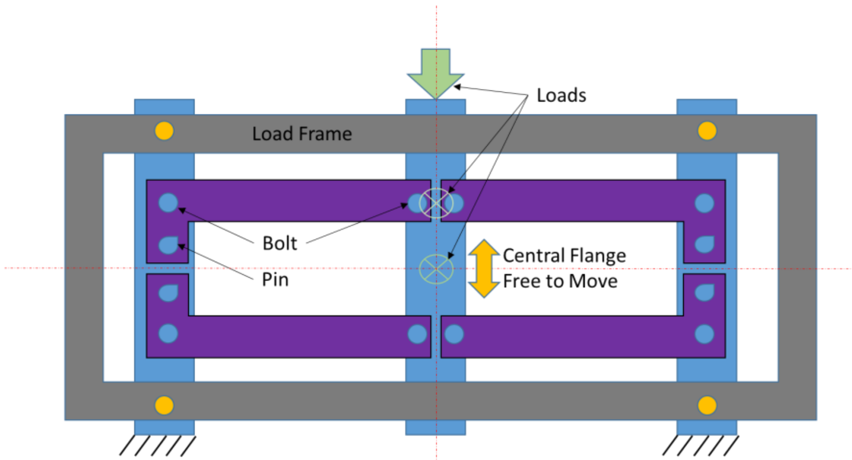

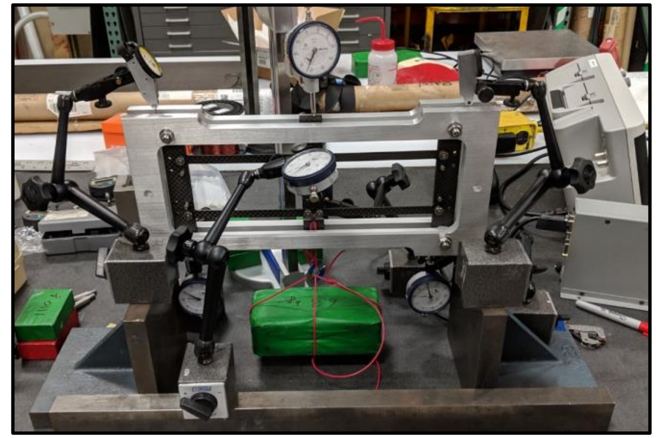

- Prototypes designed to verify the 'real' stiffness of non-bonded components and the strength of the most critical components/interfaces
  - **Static** and **dynamic** testing (damping)
  - **Local compliance** due to bolted connections can significantly affect the overall performances
    - Function of the applied **prestress** and **friction**
    - Can stabilize after a few cycles for low **prestress** conditions

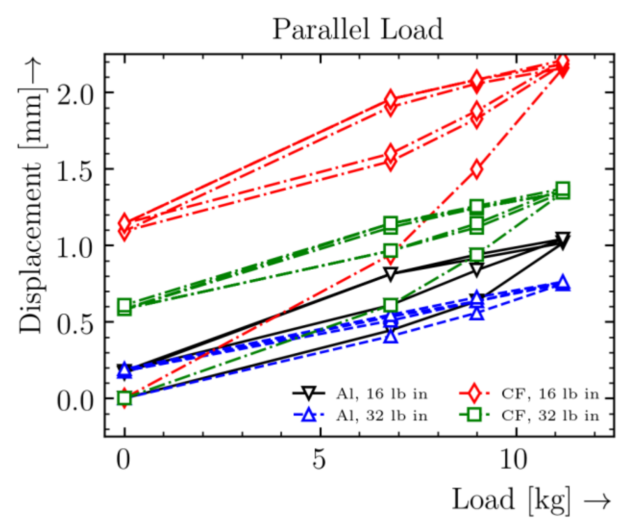

BERKELEY LAB

Strength Considerations

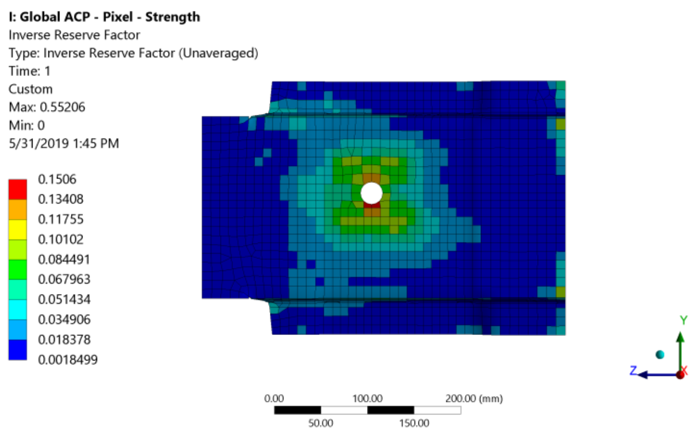

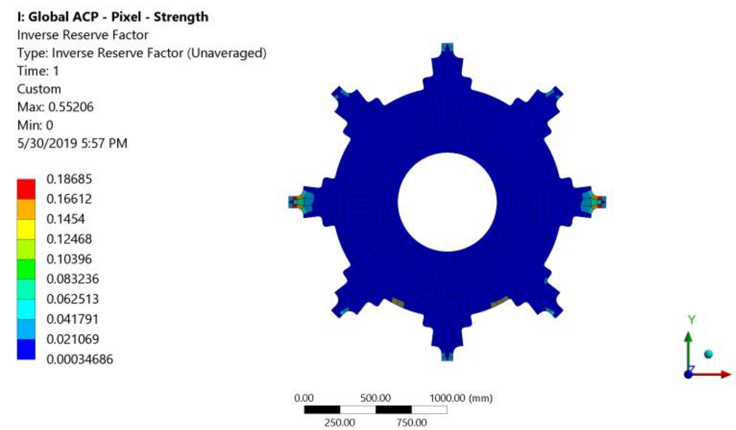

- **Maximum strain** as laminate failure criteria
  - **Fiber failure** mostly relevant
  - Special submodels to test for specific extreme load-cases
- **Inverse reserve factor** used to have a 'single' failure plot (L_a is the applied load, L_f the failure load):

$$IRF = \frac{1}{SF} = \frac{L_a}{L_f}$$

- Critical joints verified **experimentally**

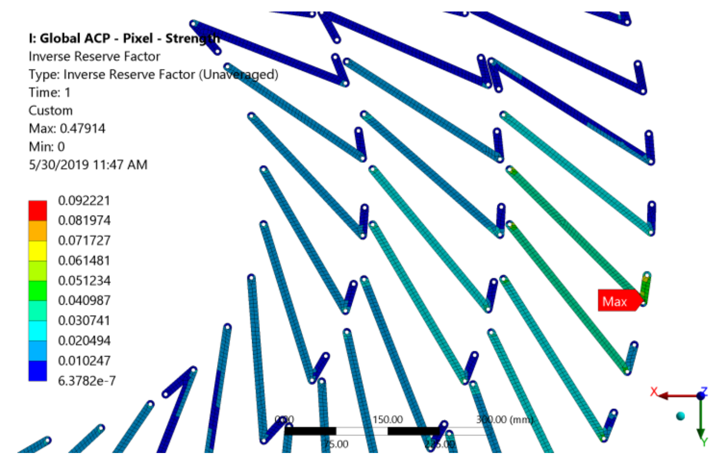

BERKELEY LAB

Outline

- Introduction
- The ATLAS Inner Tracker Design
- Experimental Design Verification
- Debonding models
- Conclusion

Experimental Tests - Strength

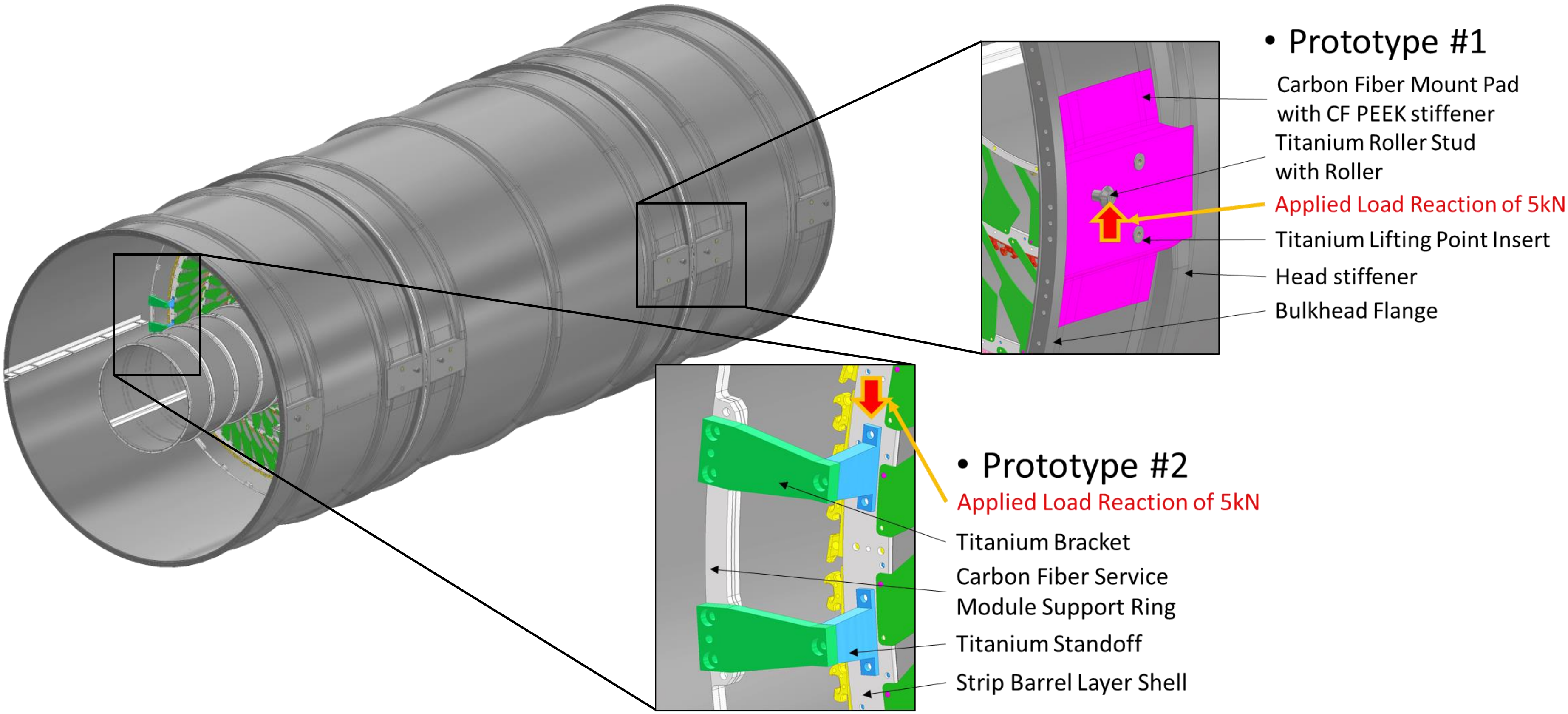

Prototypes used to verify critical components along the main load path:

- P1: **Mount pads** support the detector on the vessel **rails**
- P2: **Brackets** support the strip barrel and the pixel on the **outer cylinder flanges**

Mount Pad Test Setup

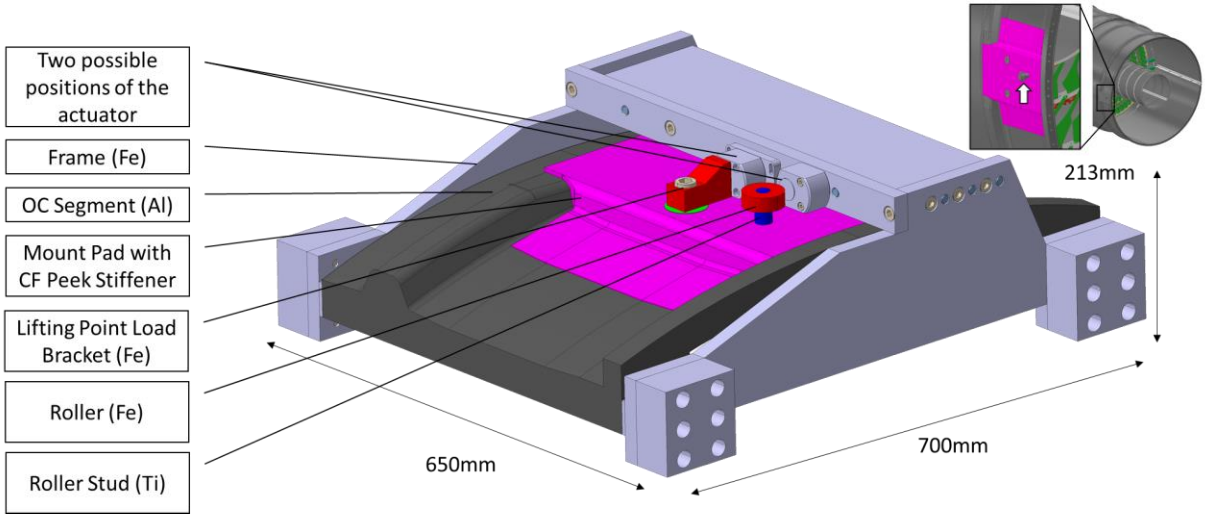

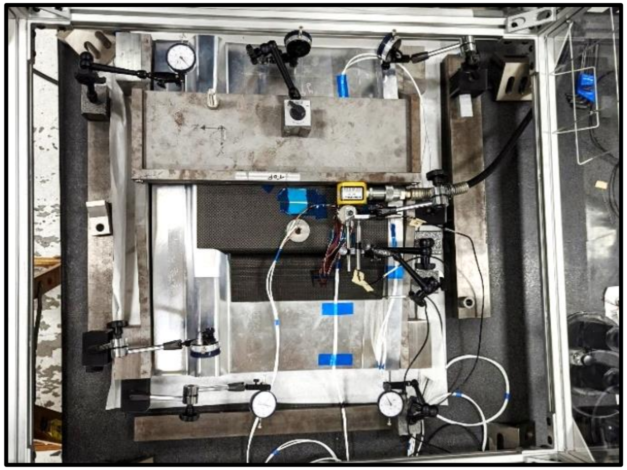

Physical ‘sub-model’ including an aluminium (~stiffness to ‘black aluminum’) reproduction of the outer cylinder

- Two actuator positions to test for **lifting** and **operation**
- **Sensors** installed:
  - **Dial gauges** to check frame motion
  - **LVDTs** to measure the displacement at the stud and of the outer cylinder segment
  - **Strain gauges** (half-bridge and rosettes) on the roller stud and the mount pad

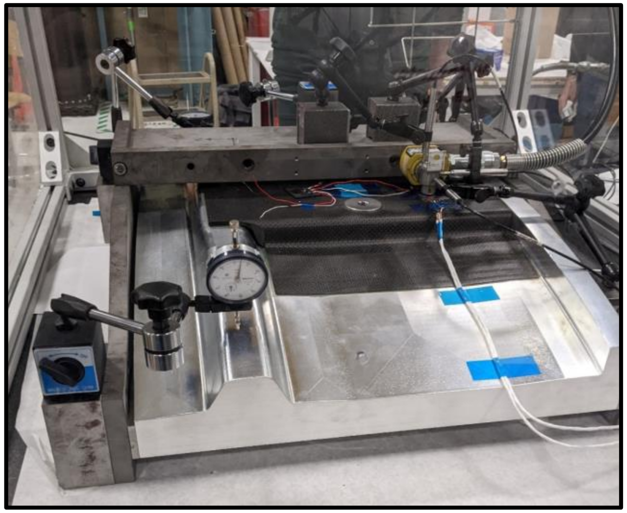

BERKELEY LAB

Test History – Part 1

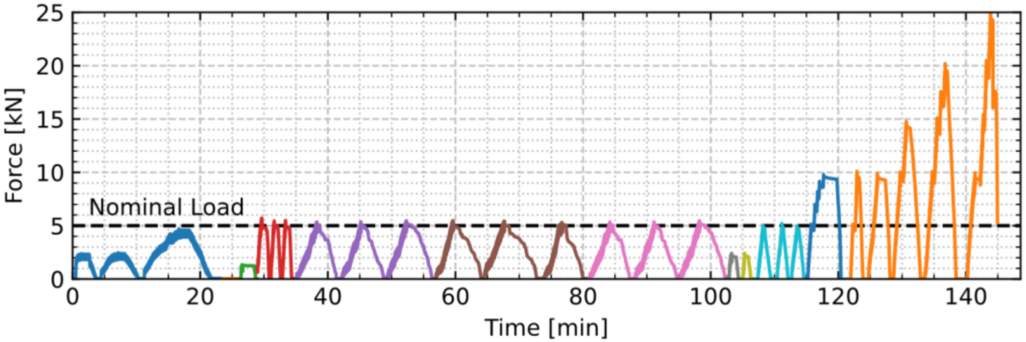

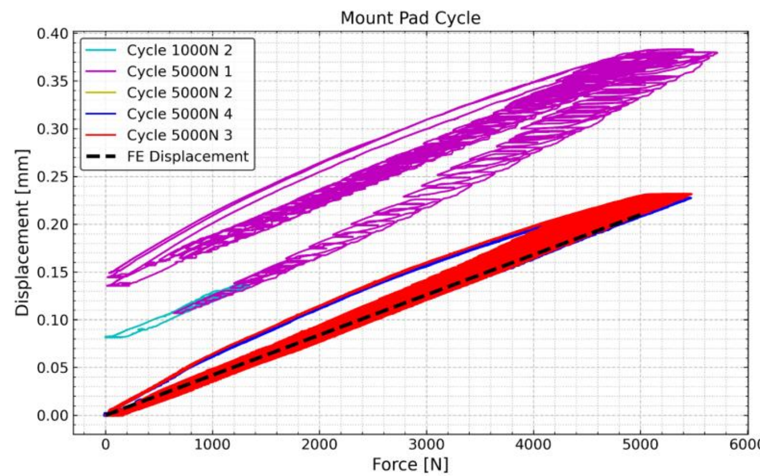

Cycling around the nominal load to verify the real **stiffness** of the system

- **Hysteresis** loops caused by the pressure regulation system
- Good match of meas. **displacement** with FE prediction – **performance** as **expected**
- SG system will be used for **SHM** purposes during **detector assembly**
- Measured **strain** follows the FE slope up to ~1.7 kN, then deviates: the stud rotation moves the load application point

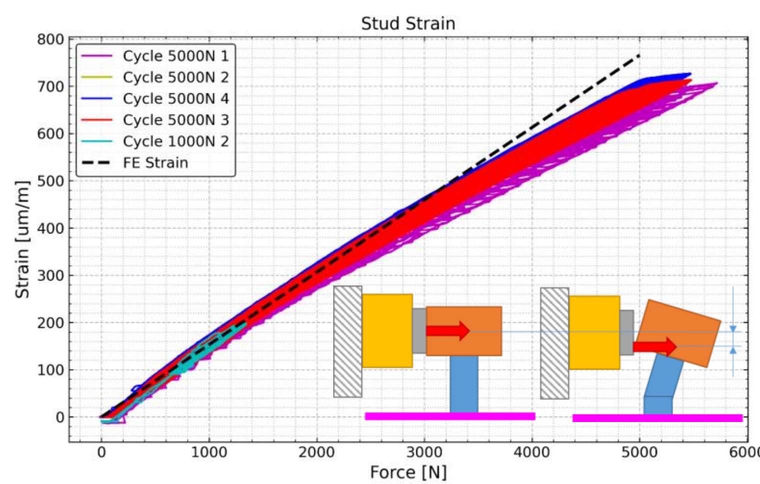

Test History – Part 2

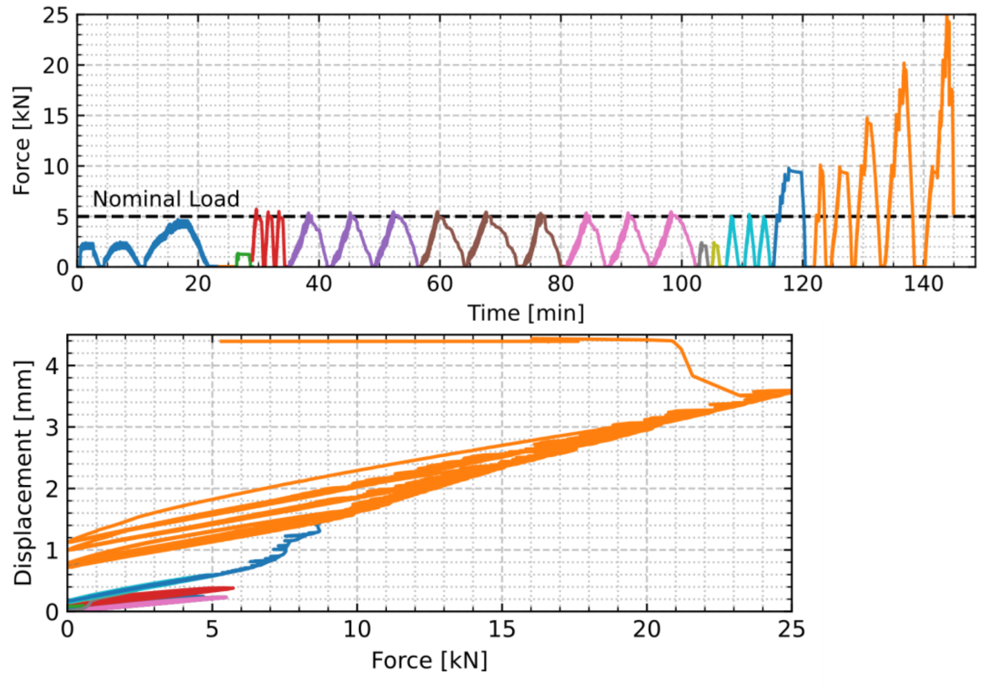

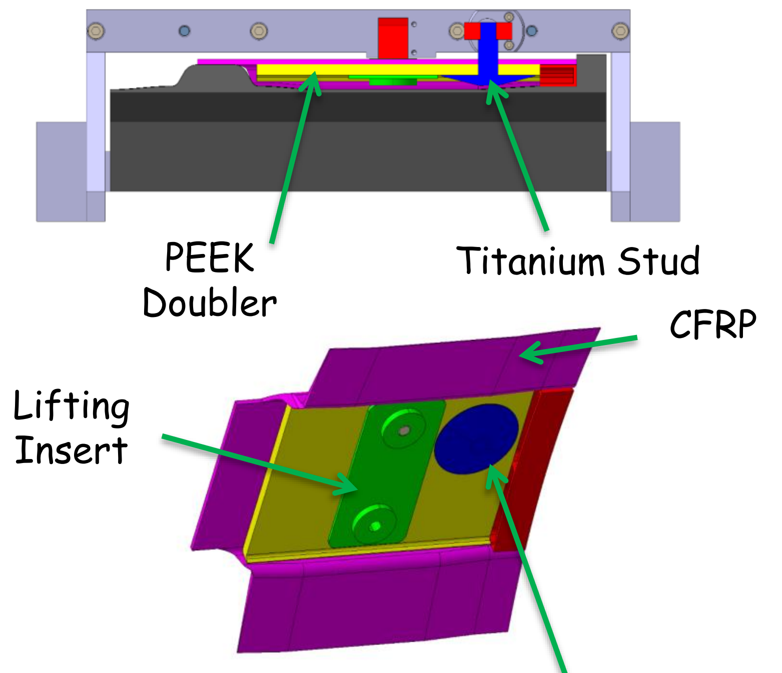

Ramps with gradual **load** increase, checking for stiffness **degradation** and **failure**

- Abrupt failure at 23 kN
  - **Bonding** (EA 9394) between mount pad and **stud** insert failed
  - Large margin (>4) over applied loads: **design** is **ok**!
  - Still useful to try to match it with more advanced models…

BERKELEY LAB

Outline

- Introduction
- The ATLAS Inner Tracker Design
- Experimental Design Verification
- Debonding models
- Conclusion

Debonding Models

Crack propagation approaches can be used to simulate debonding in FEM:

- ‘Manually’ **kill contact** elements (birth/death)
- Virtual Crack Closure Technique (**VCCT**)
- **Plastic glue** models – can be combined with birth/death
- Cohesive zone model (**CZM**)
- **SMART** crack growth (K_I/J-integral + adaptive re-meshing)
- **XFEM** – enriched elements

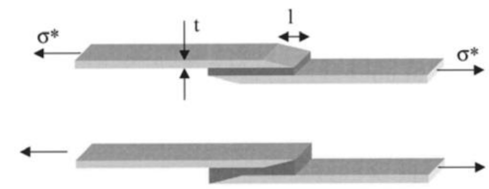

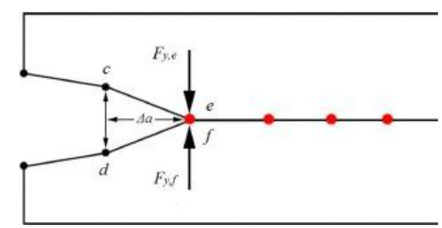

CZM seems particularly suited for the problem at hand:

- We already know the failure location/propagation
- Glue stiffness can be introduced easily

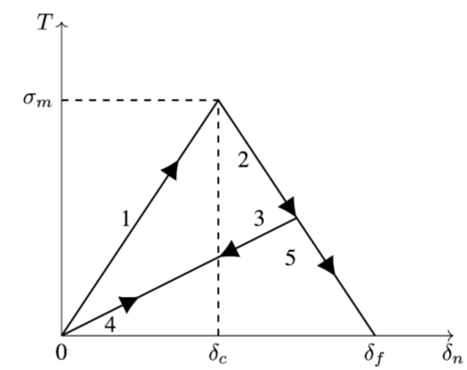

Material **properties** required:

- Glue **elastic** properties (E, nu) and **thickness**
- Elastic and shear **strength**
- **Fracture** energy release rate for different modes (G_{IC}, G_{IIC})

BERKELEY LAB

Cohesive Zone Models

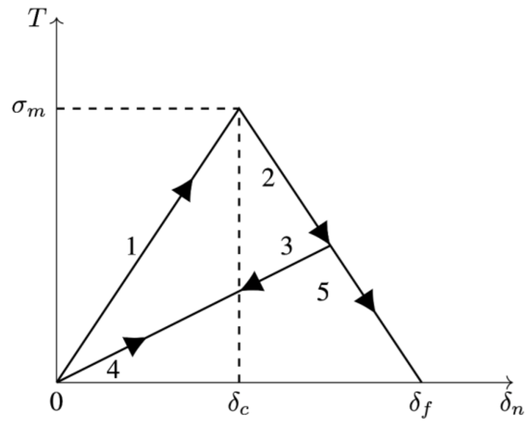

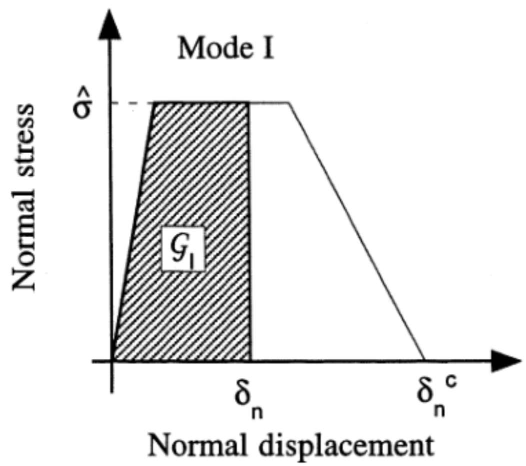

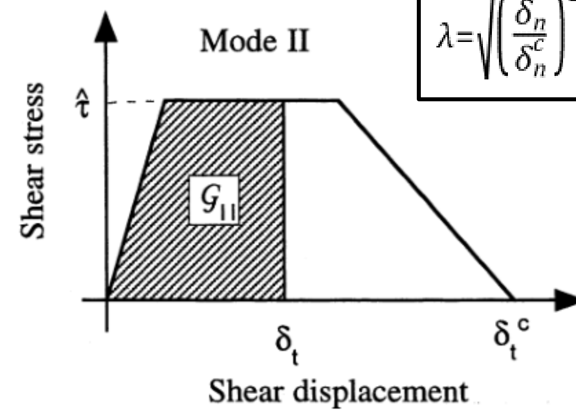

$$\lambda=\sqrt{\left(\frac{\delta_n}{\delta_n^c}\right)^2+\beta^2\left(\frac{\delta_t}{\delta_t^c}\right)^2}$$

- **Cohesive** zone **model**:
  - Initial slope dictated by the **glue modulus** and **thickness**
  - δ_c is the displacement at the **damage** '**start**'
    - **Degraded stiffness** for damaged interfaces
  - δ_f is the displacement at the **debonding completion**
  - Damage defined as: $\lambda = \frac{\delta-\delta_c}{\delta_f}$ for $\delta > \delta_c$, 0 otherwise
  - Total area below the curve equal to the **energy release rate** G

CZM - Examples

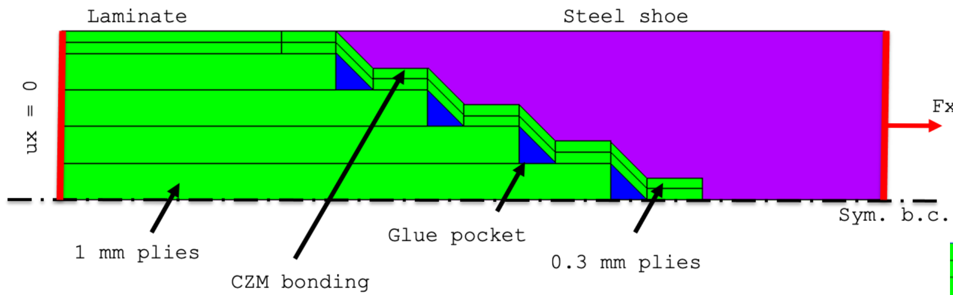

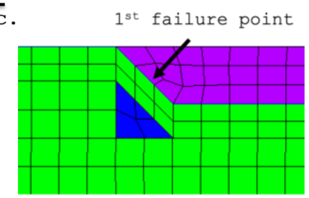

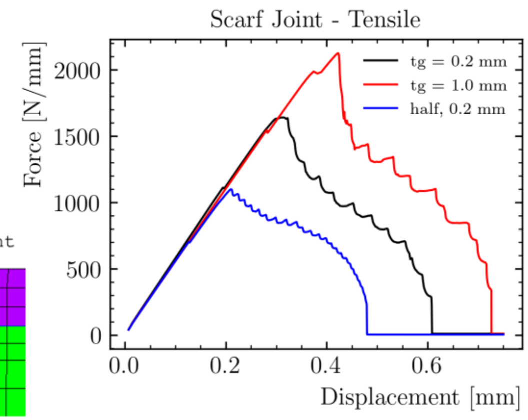

A scarf joint failure model for DUNE

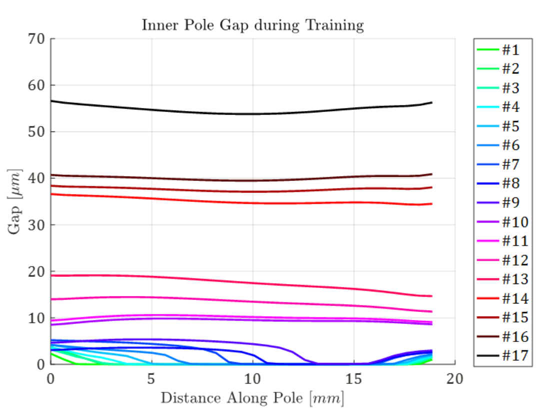

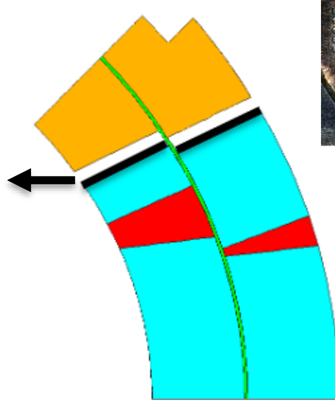

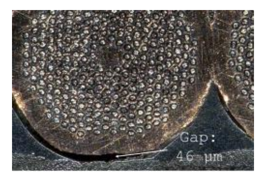

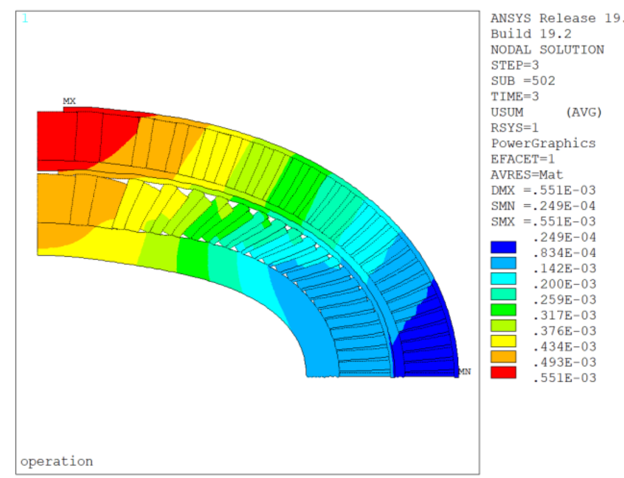

Superconducting Magnets Models
See for example G. Vallone, P. Ferracin, SUST (2017)

BERKELEY LAB

Typical Adhesive Properties

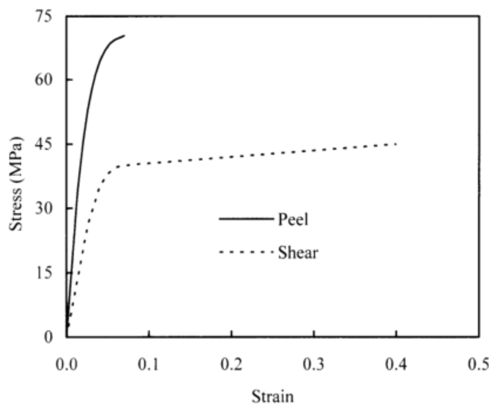

Figure 2.16 Stress-strain curves for FM300-K film adhesive [53]

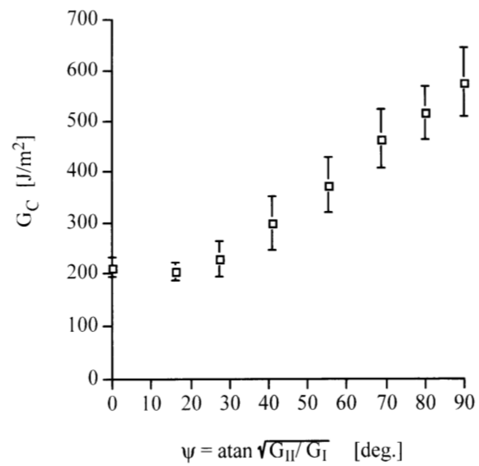

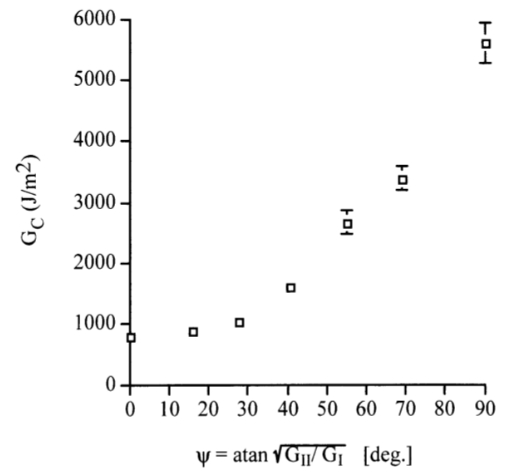

- Tensile **strength** of adhesive is usually lower than 100 MPa (50 MPa for shear)
  - **Common** values around 70 MPa tensile, 35 MPa shear
- **Tresca** criterion seems to apply on most adhesives (shear = ½ tensile)
- $G_c(\Psi)$ curves measured on different adhesive systems (Cybond 4523GB, Permabond ESP 310) suggest that roughly: $\mathbf{G_{IIc} \sim 3G_{Ic}}$

Analytical Model Description (1)

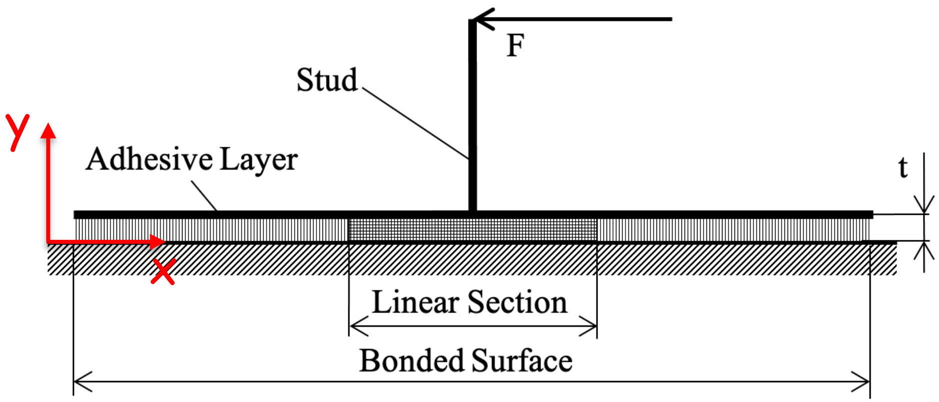

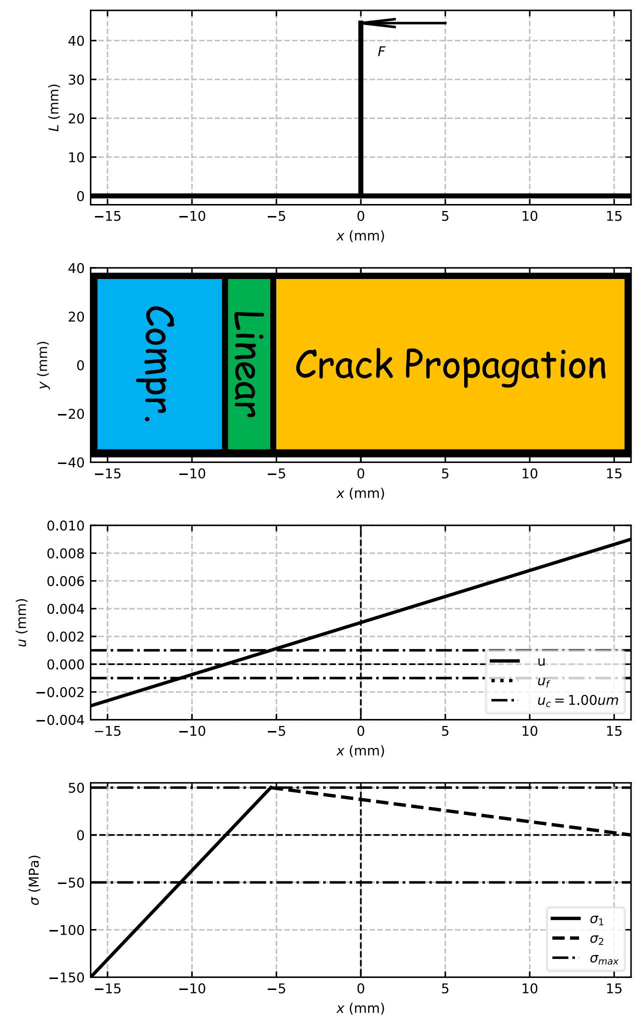

Analytical model of the (simplified) bonded joint:

- All the deformation is within the glue, the adherents are assumed as infinitely rigid
- All the surrounding elements are neglected – the mount pad surface is assumed to be fixed
- The insert is rotating with respect to the mount pad surface

- **Normal displacement** (y-direction) across the interface:

$$u(x) = u_c + \beta(x - x_c)$$

- **Glue** introduced with a **cohesive** zone model
  - Limited to the stud area

Analytical Model Description (2)

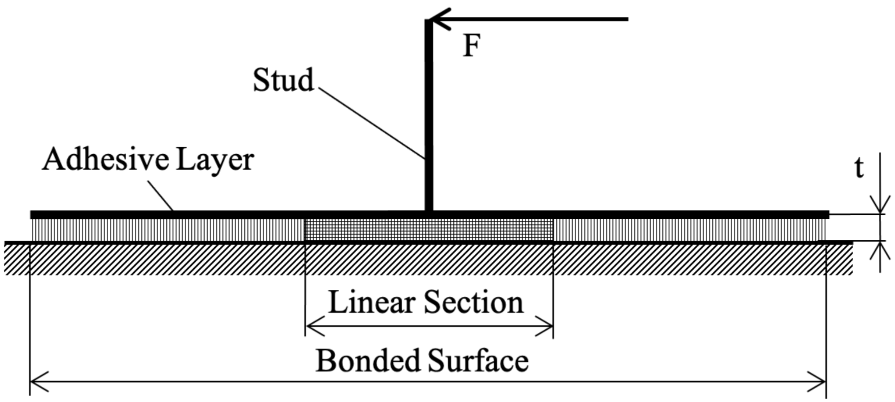

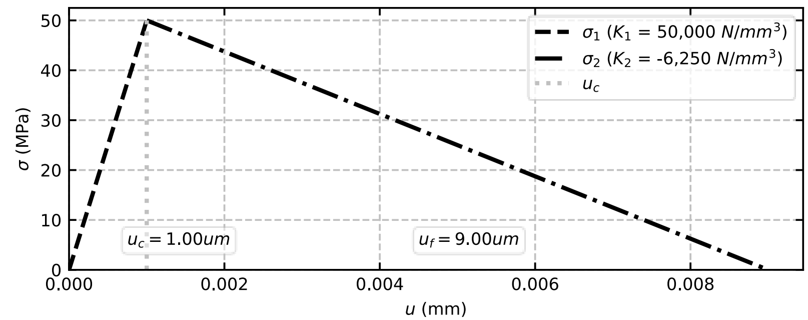

- **Equilibrium** equations can be solved in close form for a rectangular bonded surface, only numerically for circular

$\int_A \sigma(x)\, dA = 0$ and $\int_A \sigma(x)\, x\, dA = FL$

$$\int_{A_1} K_1\, u(x)\, dA_1 + \int_{A_2} K_2 \left(u(x) - u_f\right) dA_2 = 0$$

$$\int_{A_1} K_1\, u(x)\, x\, dA_1 + \int_{A_2} K_2 \left(u(x) - u_f\right) x\, dA_2 = FL$$

- Applied **force** :

$$F(x_c) = f(u_c, u_f, K_1, K_2, R, L, t)$$

- Separate solution needed when part of the bonding is completely failed

Property	Value
Adhesive modulus	$E = 5000 MPa$
Adhesive Normal Contact Stress	$\sigma_{max} = 50 MPa$
Critical Fracture Energy for Normal Separation	$G = 200 \cdot 10^{-3} mJ/mm^2$
Adhesive thickness	$t = 0.1 mm$

For a rectangular bonding:

$$F(x_c) = D K_2^2 (u_c - u_f)(R - x_c)^4 + D K_1^2\, u_c (R + x_c)^4 + \\ + D K_1\, K_2 (R^2 - x_c^2)(7\, R^2 (2u_c - u_f) - 8\, R\, u_f\, x_c \\ + (2u_c - u_f) x_c^2)$$

With:

$$D = \frac{a}{6\, L\, (-K_2 (R - x_c)^2 + K_1 (R + x_c)^2)}$$

Analytical Model Results (1)

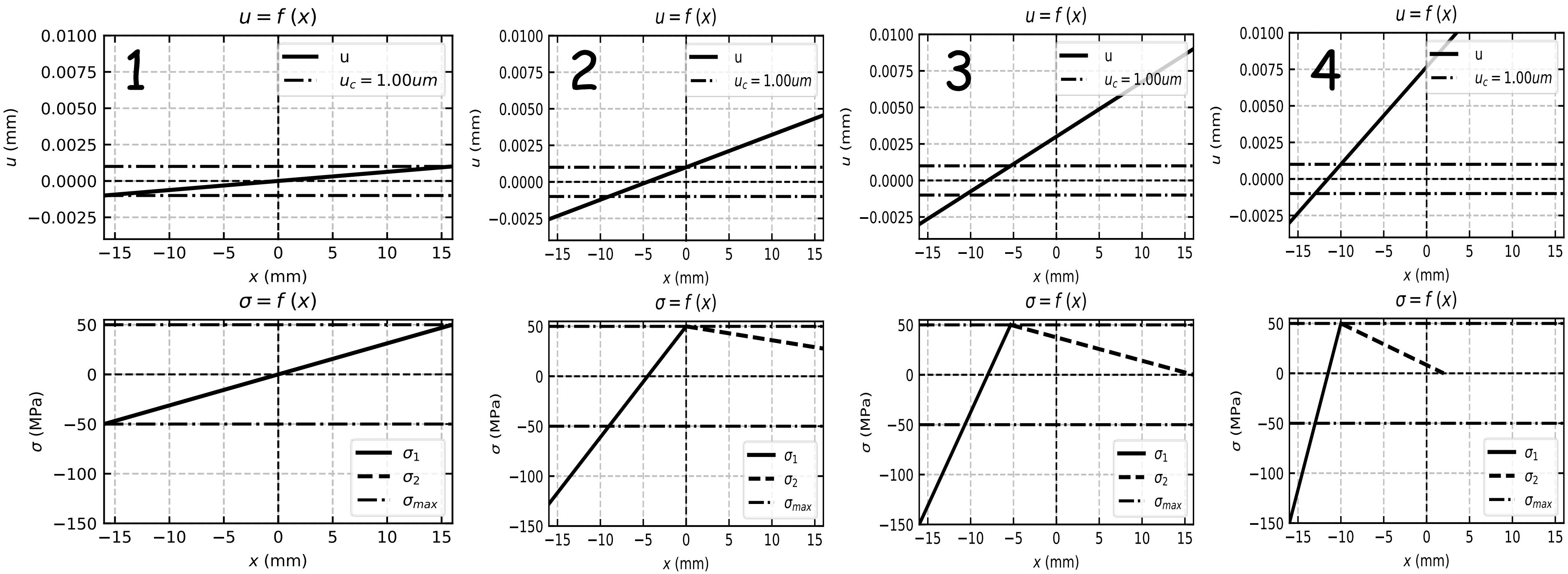

- **Displacement** and **stress** along the bonding line:
  1. Linear regime
  2. Plastic deformation in the glue
  3. Failure onset at the right edge
  4. Partially failed glue

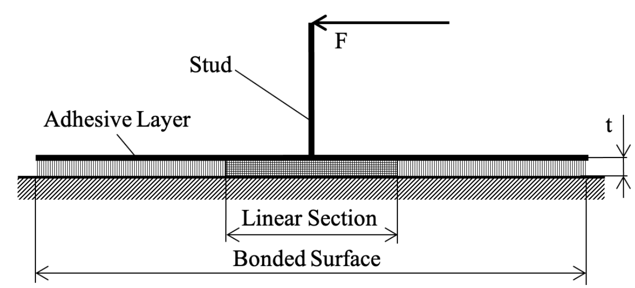

BERKELEY LAB

Analytical Model Results (2)

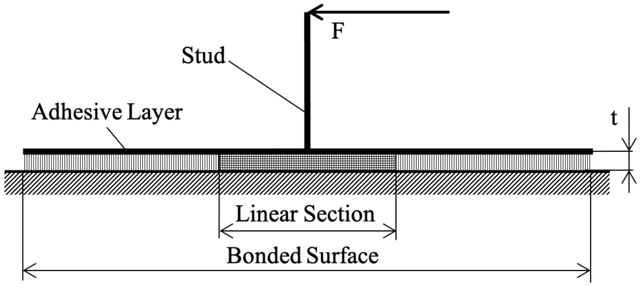

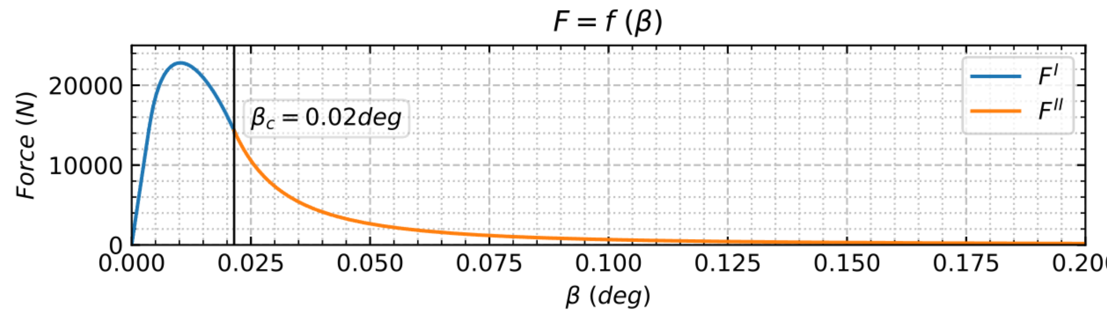

- **Separate solutions**: before and after onset of complete failure region
  - Blue curve: initial **linear** regime, then bonding **damaged**, but no failure
  - Orange curve: part of the contact failed – **separation** occurring between the insert and the laminate
- Bonding '**degradation**' starts at 14.3 kN
  - Stiffness (performance) of the system decreases
- While the damage in the bonded region is growing, the force also increases up to the ultimate value of **22.8 kN**

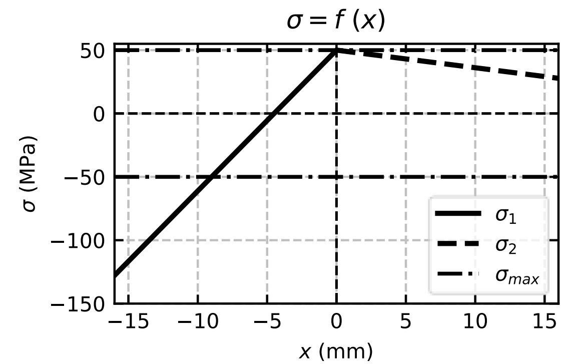

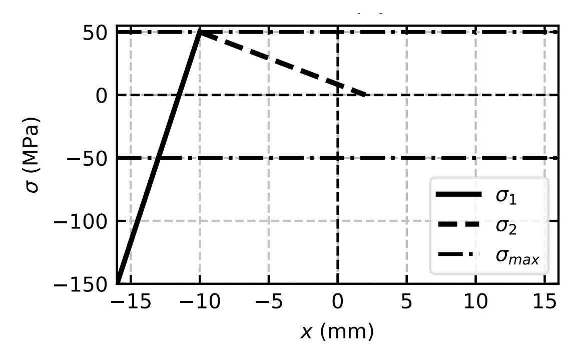

BERKELEY LAB

Simplified FE Model of the Bonded Region

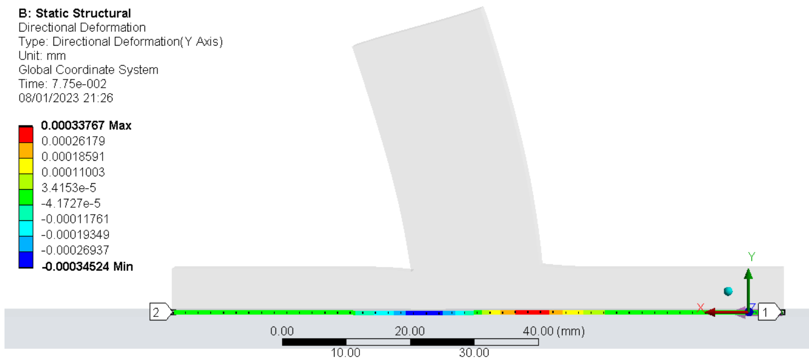

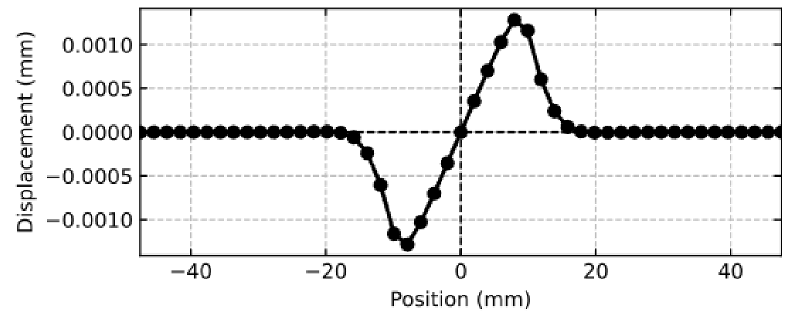

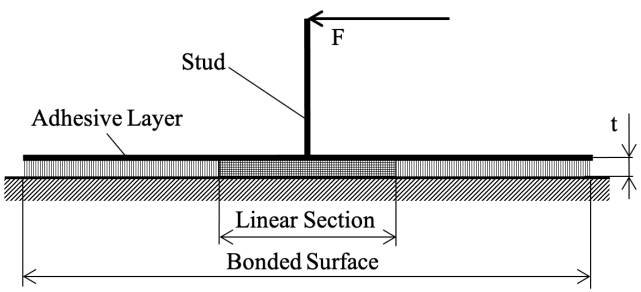

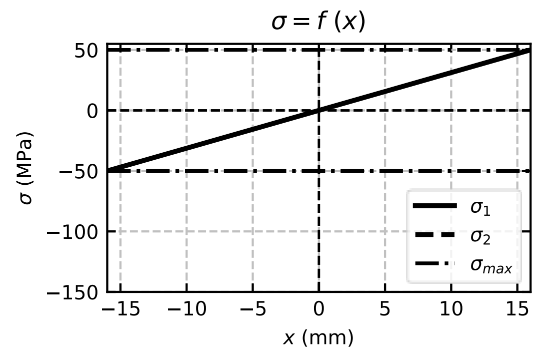

- **Simplified** FE **model** built to verify the **assumptions** of the analytical model
  - Titanium insert bonded to a infinitely rigid fixed plane
- What is the ‘real’ **contact surface deformation** along the bonding?
  - Linear assumption within the stud width seems reasonable, but neglects the ‘negative ramp’ region

BERKELEY LAB

Mount Pad FE Model

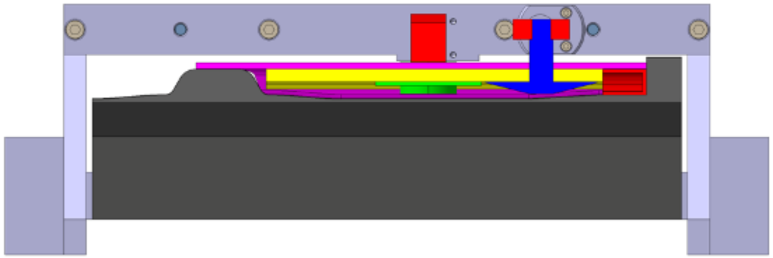

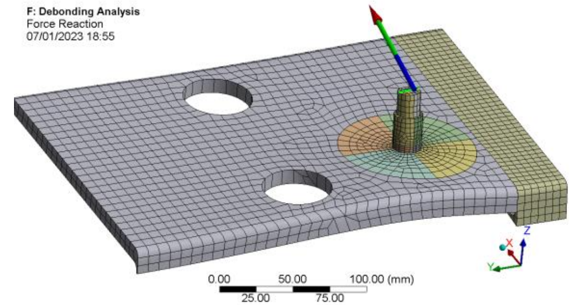

FE failure submodel – some **simplifications** in order to reduce the computational load

- **Computed failure load**: 19.7 kN
- This is lower (15%) than the measured value:
  - Model **compliance** reduced w.r.t the experiment due to simplifications
  - **Uncertainty** in actual **bond properties** (from analogy with literature)

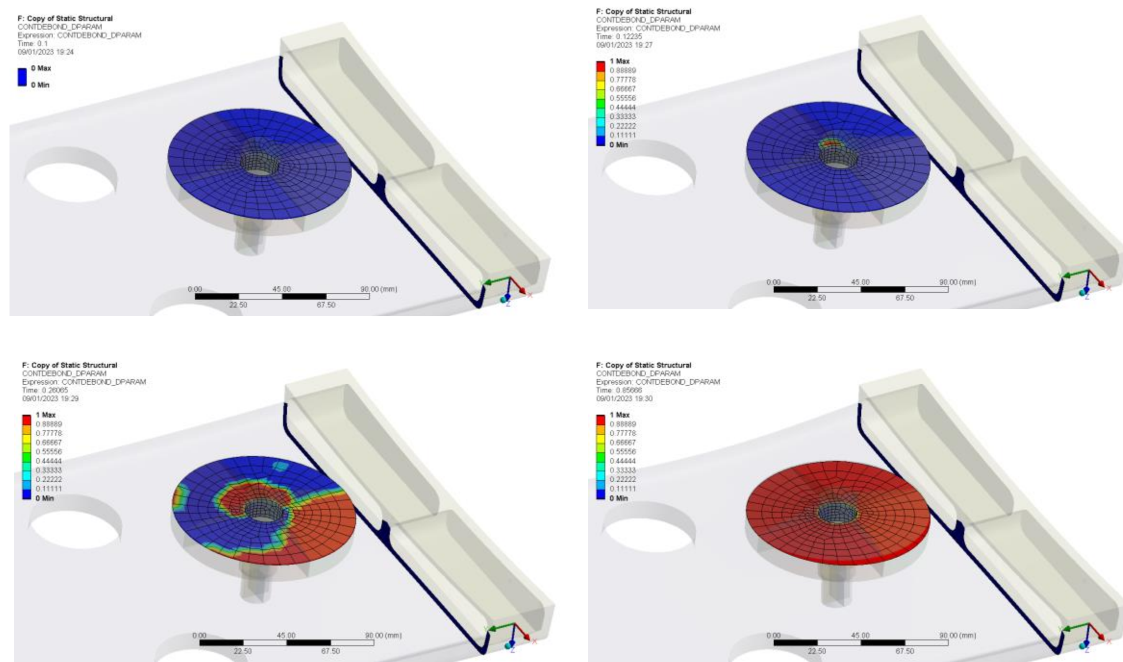

BERKELEY LAB

Outline

- Introduction
- The ATLAS Inner Tracker Design
- Experimental Design Verification
- Debonding models
- Conclusion

Conclusion

- Global ITk **structure** relies on thin, eccentrically stiffened, **CFRP laminates**
  - Design relies extensively on finite element **modeling**
  - Designed for **stiffness**, **strength** largely **exceeds** safety **requirements**

- **Prototypes** used to verify the actual **stiffness** of non-bonded components and the **strength** of critical components along the main load path
  - The failure point of a **bonded** joint was measured (~4 times the ultimate load)
  - Different approaches implemented to simulate the failure process
  - Both FE and analytical models prediction is close to the failure load

Case	Failure Load
/	kN
Measured	23.0
Analytical Model	22.8
FE Model	19.7

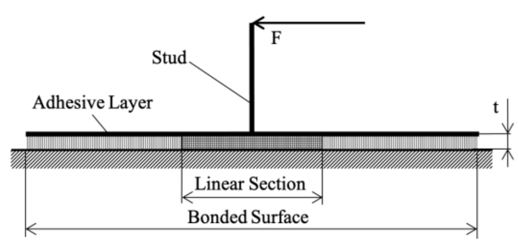

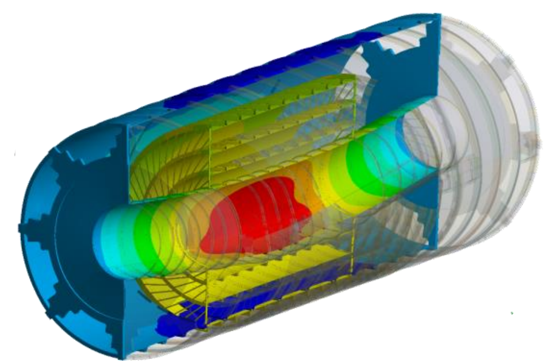

References

1. L. Gonnella, The ATLAS ITk detector system for the Phase-II LHC upgrade, Nuclear Inst. And Methods in Physics Research A, 2023, https://doi.org/10.1016/j.nima.2022.167597
2. ATLAS Collaboration. *Technical Design Report for the ATLAS Inner Tracker Pixel Detector*. Geneva, 2017. DOI: 1 0.17181/CERN.FOZZ.ZP3Q. URL: http://cds.cern.ch/record/2285585.
3. ATLAS Collaboration. *Technical Design Report for the ATLAS Inner Tracker Strip Detector*. Geneva, 2017. URL: http://cds.cern.ch/record/2257755.
4. Vallone, Giorgio et al., "*Outer Cylinder, Design Report for PRR*". CERN EDMS No. 2048058, Technical Report AT2-IG-ER-0001, https://edms.cern.ch/document/2391486/5
5. Tong, Liyong and Soutis, Costas. Recent Advances in Structural Joints and Repairs for Composite Materials. Springer Dordrecht, 2003. , https://doi.org/10.1007/978-94-017-0329-1
6. Henkel Corporation, Hysol® EA 9394 Epoxy Paste Adhesive Properties
7. Guess, T. R., Reedy, E. D. and M. E. Stavig. *Mechanical properties of Hysol EA-9394 structural adhesive*. No. SAND-95-0229. Sandia National Lab.(SNL-NM), Albuquerque, NM (United States), 1995.
8. Barenblatt, Grigory Isaakovich. "*The Mathematical Theory of Equilibrium Cracks in Brittle Fracture*". 1962. Advances in Applied Mechanics, Volume 7, pp .5-129.
9. Dugdale, Donald Stephen. "*Yielding of Steel Sheets Containing Slits*". 1960. Journal of the Mechanics and Physics of Solids, Volume 8, pp. 100-104.
10. Park, Kyoungsoo and Paulino, Glaucio H. "*Cohesive Zone Models: A Critical Review of Traction-Separation Relationships Across Fracture Surfaces*". November 2011. Applied Mechanics Reviews, Volume 64.

Thanks for your attention!

Contact:
gvallone@lbl.gov
ecanderssen@lbl.gov
martin.janda@cern.ch

BERKELEY LAB